A comparison of design-based and model-based approaches for finite population spatial sampling and inference.

Michael Dumelle*[,a], Matt Higham[b], Jay M. Ver Hoef[c], Anthony R. Olsen[a], Lisa Madsen[d]

[a] *United States Environmental Protection Agency, 200 SW 35th St, Corvallis, Oregon, 97333*
[b] *St. Lawrence University Department of Mathematics, Computer Science, and Statistics, 23 Romoda Drive, Canton, New York, 13617*
[c] *Marine Mammal Laboratory, Alaska Fisheries Science Center, National Oceanic and Atmospheric Administration, Seattle, Washington, 98115*
[d] *Oregon State University Department of Statistics, 239 Weniger Hall, Corvallis, Oregon, 97331*

Abstract

1. The design-based and model-based approaches to frequentist statistical inference rest on fundamentally different foundations. In the design-based approach, inference relies on random sampling. In the model-based approach, inference relies on distributional assumptions. We compare the approaches in a finite population spatial context.
2. We provide relevant background for the design-based and model-based approaches and then study their performance using simulated data and real data. The real data is from the United States Environmental Protection Agency's 2012 National Lakes Assessment. A variety of sample sizes, location layouts, dependence structures, and response types are considered. The population mean is the parameter of interest, and performance is measured using statistics like bias, squared error, and interval coverage.
3. When studying the simulated and real data, we found that regardless of the strength of spatial dependence in the data, the generalized random tessellation stratified (GRTS) algorithm, which explicitly incorporates spatial locations into sampling, tends to outperform the simple random

*Corresponding Author: Michael Dumelle (Dumelle.Michael@epa.gov)

sampling (SRS) algorithm, which does not explicitly incorporate spatial locations into sampling. We also found that model-based inference tends to outperform design-based inference, even for skewed data where the model-based distributional assumptions are violated. The performance gap between design-based inference and model-based inference is small when GRTS samples are used but large when SRS samples are used, suggesting that the sampling choice (whether to use GRTS or SRS) is most important when performing design-based inference.

4. There are many benefits and drawbacks to the design-based and model-based approaches for finite population spatial sampling and inference that practitioners must consider when choosing between them. We provide relevant background contextualizing each approach and study their properties in a variety of scenarios, making recommendations for use based on the practitioner's goals.

Keywords

Design-based inference; Finite population block kriging (FPBK); Generalized random tessellation stratified (GRTS) algorithm; Local neighborhood variance estimator; Model-based inference; Restricted maximum likelihood (REML) estimation; Spatially balanced sampling; Spatial covariance

1. Introduction

When data cannot be collected for all units in a population (population units), data are collected on a subset of the population units – this subset is called a sample. There are two general approaches for using samples to make frequentist statistical inferences about a population: design-based and model-based. In the design-based approach, inference relies on randomly assigning some population

units to be in the sample (random sampling). Alternatively, in the model-based approach, inference relies on distributional assumptions about the underlying data-generating stochastic process (superpopulation). Each paradigm has a deep historical context (Sterba, 2009) and its own set of benefits and drawbacks (Brus and De Gruijter, 1997; Hansen et al., 1983). In this manuscript, we compare design-based and model-based approaches for finite population spatial sampling and inference.

Spatial data are data that have some sort of spatial index (usually specified via coordinates). De Gruijter and Ter Braak (1990) and Brus and DeGruijter (1993) give early comparisons of design-based and model-based approaches for spatial data, quashing the belief that design-based approaches could not be used for spatially correlated data. Since then, there have been several general comparisons between design-based and model-based approaches for spatial data (Brus and De Gruijter, 1997; Brus, 2021; Ver Hoef, 2002, 2008). Cooper (2006) reviews the two approaches in an ecological context before introducing a "model-assisted" variance estimator that combines aspects from each approach. In addition to Cooper (2006), there has been substantial research and development into estimators that use both design-based and model-based principles (see e.g., Sterba (2009) and Cicchitelli and Montanari (2012), and for Bayesian approaches, see Chan-Golston et al. (2020) and Hofman and Brus (2021)).

While comparisons between design-based and model-based approaches have been studied in spatial contexts, our contribution is comparing design-based approaches specifically built for spatial data to model-based approaches. Though the broad comparisons we draw between design-based and model-based approaches generalize to finite and infinite populations, we focus on finite populations. A finite population contains a finite number of population units (we assume the finite number is known) – an example is lakes (treated as a whole

with the lake centroid representing location) in the conterminous United States. An infinite population contains an infinite number of population units – an example is locations within a single lake.

The rest of the manuscript is organized as follows. In Section 1.1, we introduce and provide relevant background for design-based and model-based approaches to finite population spatial sampling and inference. In Section 2, we describe how we intend to compare performance of the approaches using simulated and real data. The real data is from the United States Environmental Protection Agency's 2012 National Lakes Assessment (NLA) (USEPA, 2012). In Section 3, we present analysis results for the simulated data and real data. And in Section 4, we end with a discussion and provide directions for future research.

1.1. Background

The design-based and model-based approaches incorporate randomness in fundamentally different ways. In this section, we describe the role of randomness for each approach and the subsequent effects on statistical inferences for spatial data.

1.1.1. Comparing Design-Based and Model-Based Approaches

The design-based approach assumes the population is fixed. Randomness is incorporated via the selection of population units according to a sampling design. A sampling design assigns a probability of selection to each sample (subset of population units). Some examples of commonly used sampling designs include simple random sampling, stratified random sampling, and cluster sampling. The inclusion probability of a population unit is calculated by summing each sample's probability of selection over all samples that contain the population unit. Inclusion probabilities are often used when selecting samples and estimating population parameters.

When samples are chosen in a manner such that the layout of sampled units reflects the layout of the population units, we call the resulting sample spatially balanced. By "reflecting the layout of the population units", we mean that if population units are concentrated in specific areas, the units in the sample should be concentrated in the same areas. Because spatially balanced samples reflect the layout of the population units, they are not necessarily spread out in space in some equidistant manner. One method of selecting spatially balanced samples is the generalized random tessellation stratified (GRTS) algorithm (Stevens and Olsen, 2004), which we discuss in more detail in Section 1.1.2. To quantify the spatial balance of a sample, Stevens and Olsen (2004) proposed loss metrics based on Voronoi polygons (i.e., Dirichlet Tessellations).

Fundamentally, the design-based approach combines the randomness of the sampling design with the data collected via the sample to justify the estimation and uncertainty quantification of fixed, unknown parameters of a population (e.g., a population mean). Treating the data as fixed and incorporating randomness through the sampling design yields estimators having very few other assumptions. Confidence intervals for these types of estimators are typically derived using limiting arguments that incorporate all possible samples. Sample means, for example, are asymptotically normal (Gaussian) by the central limit theorem (under some assumptions). If we repeatedly select samples from the population, then 95% of all 95% confidence intervals constructed from a procedure with appropriate coverage will contain the true fixed population mean. Särndal et al. (2003) and Lohr (2009) provide thorough reviews of the design-based approach.

The model-based approach assumes the population is a random realization of a data-generating stochastic process. Randomness is formally incorporated through distributional assumptions on this process. Strictly speaking, randomness need not be incorporated through random sampling, though Diggle et al. (2010)

warn against preferential sampling. Preferential sampling occurs when the process generating the data locations and the process being modeled are not independent of one another. To guard against preferential sampling, model-based approaches can implement some form of random sampling. It is common, however, for model-based approaches to sample non-randomly. When model-based approaches do implement random sampling, the inclusion probabilities are ignored when analyzing the sample (in contrast to the design-based approach, which relies on these inclusion probabilities to analyze the sample).

Instead of estimating fixed, unknown population parameters, as in the design-based approach, often the goal of model-based inference is to predict the value of a realized variable. For example, suppose the realized mean of all population units (the realized population mean) is the variable of interest. Instead of a fixed, unknown mean, we are predicting the value of the mean, a random variable. Prediction intervals are then derived using assumptions of the data-generating stochastic process. If we repeatedly generate realizations from the same process and select samples, then 95% of all 95% prediction intervals constructed from a procedure with appropriate coverage will contain their respective realized means. Cressie (1993) and Schabenberger and Gotway (2017) provide thorough reviews of model-based approaches for spatial data. In Fig. 1, we provide a visual comparison of the design-based and model-based approaches (Ver Hoef (2002) and Brus (2021) provide similar figures). Fig. 1 contrasts the design-based approach with a fixed population and random sampling to the model-based approach with random populations and non-random sampling.

1.1.2. Spatially Balanced Design and Analysis

We previously mentioned that the design-based approach can be used to select spatially balanced samples. Spatially balanced samples are useful because parameter estimates from these samples tend to vary less (be more precise)

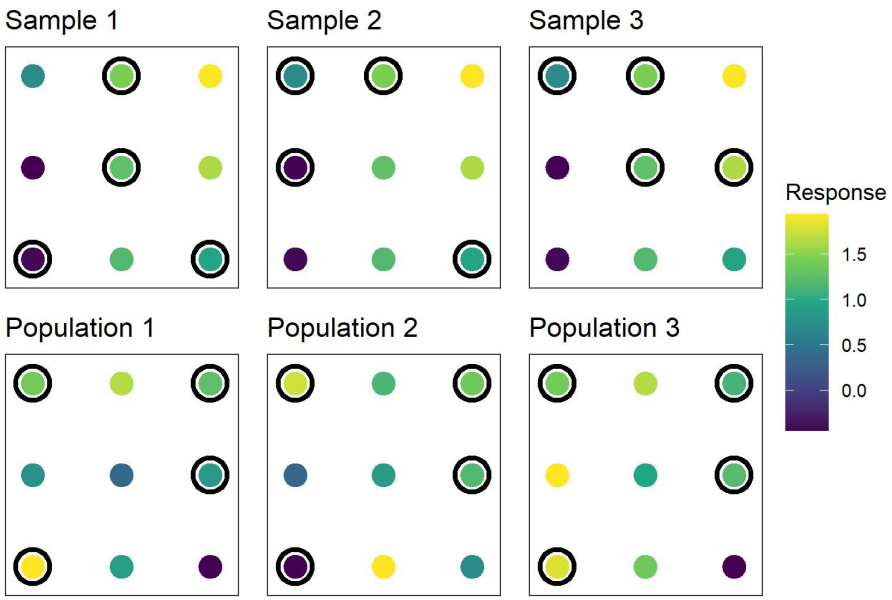

Figure 1: A visual comparison of the design-based and model-based approaches. In the top row, the design-based approach is highlighted. There is one fixed population with nine population units and three random samples of size four (points circled are those sampled). The response values at each site are fixed. In the bottom row, the model-based approach is highlighted. There are three realizations of the same data-generating stochastic process that are all sampled at the same four locations. The response values at each site are random.

than parameter estimates from samples lacking spatial balance (Barabesi and Franceschi, 2011; Benedetti et al., 2017; Grafström and Lundström, 2013; Robertson et al., 2013; Stevens and Olsen, 2004; Wang et al., 2013). The first spatially balanced sampling algorithm to see widespread use was the generalized random tessellation stratified (GRTS) algorithm (Stevens and Olsen, 2004). After the GRTS algorithm was developed, several other spatially balanced sampling algorithms emerged, including stratified sampling with compact geographical strata (Walvoort et al., 2010), the local pivotal method (Grafström et al., 2012; Grafström and Matei, 2018), spatially correlated Poisson sampling (Grafström, 2012), balanced acceptance sampling (Robertson et al., 2013), within-sample-distance sampling (Benedetti and Piersimoni, 2017), and Halton iterative partitioning sampling (Robertson et al., 2018). In this manuscript, we select spatially balanced samples using the GRTS algorithm because it is readily available in the `spsurvey` **R** package (Dumelle et al., 2022) and naturally accommodates finite and infinite sampling frames, unequal inclusion probabilities, and replacement units. Replacement units are additional population units that can be sampled when a population unit originally selected can no longer be sampled. A couple of reasons why an originally selected site can no longer be sampled include its location being physically inaccessible or it is on private land that the researcher does not have permission to access.

The GRTS algorithm selects samples by utilizing a particular mapping between two-dimensional and one-dimensional space that preserves proximity relationships. First, the bounding box of the domain is split up into four distinct, equally sized squares called level-one cells. Each level-one cell is randomly assigned a level-one address of 0, 1, 2, or 3. The set of level-one cells is denoted by $\mathcal{A}_1$ and defined as $\mathcal{A}_1 \equiv \{a_1 : a_1 = 0, 1, 2, 3\}$. Within each level-one cell, the inclusion probability for each population unit (which is

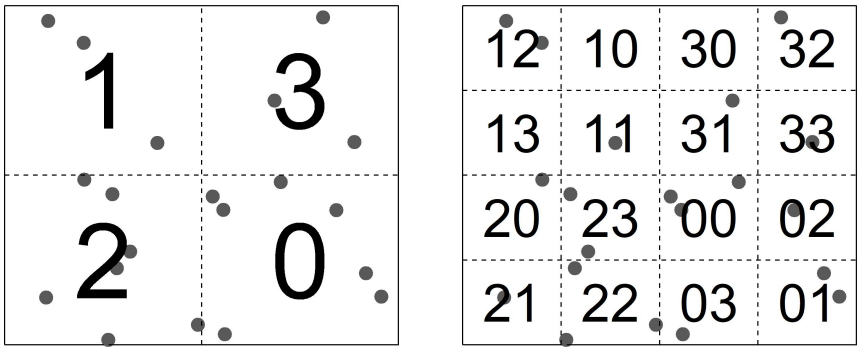

(a) Assignment of level-one cells to the spatial domain. Grey circles indicate population units.

(b) Assignment of level-two cells to the spatial domain. Grey circles indicate population units.

Figure 2: Assignment of level-one and level-two cells to the spatial domain. In (a), each level-one cells is randomly given a level-one address of 0, 1, 2, or 3. In (b), each level-two cell within each level-one cell is randomly given a level-two address of 0, 1, 2, or 3.

pre-specified) is summed, and if any of these sums exceed one, a second level of cells is added. Then each level-one cell is split into four distinct, equally sized squares called level-two cells. Each level-two cell is randomly assigned a level-two address of 0, 1, 2, or 3. The set of level-two cells is denoted by $\mathcal{A}_2$ and defined as $\mathcal{A}_2 \equiv \{a_1a_2 : a_1 = 0, 1, 2, 3; a_2 = 0, 1, 2, 3\}$. The inclusion probabilities within each level-two cell are summed, and if any of these sums exceed one, a third level of cells is added. This process continues for k steps, until all level-k cells have inclusion probability sums no larger than one. Then $\mathcal{A}_k \equiv \{a_1...a_k : a_1 = 0, 1, 2, 3; ...; a_k = 0, 1, 2, 3\}$. Figure 2 provides some intuition regarding the assignment of level-one and level-two cells.

After determining $\mathcal{A}_k$, the set is placed into hierarchical order. Hierarchical order is a numeric order that first sorts $\mathcal{A}_k$ by the level-one addresses from smallest to largest, then sorts $\mathcal{A}_k$ by the level-two addresses from smallest to largest, and so on. For example, $\mathcal{A}_2$ in hierarchical order is the set $\{00, 01, 02, 03, 10, ..., 13, 20, ..., 23, 30, ..., 33\}$. Because hierarchical ordering sorts by level-one cells, then level-two cells, and so on, population units that have

similar hierarchical addresses tend to be nearby one another in space. Next, each population unit is mapped to a one-dimensional line in hierarchical order where each population unit's inclusion probability equals its line-length. If a level-k cell has multiple population units in it, they are randomly placed within the cell's respective line segment. A uniform random variable is then simulated in $[0, 1]$ and a systematic sample is selected on the line, yielding n sample points for a sample size n. Each of these sample points falls on some population unit's line segment, and thus that population unit is selected in the sample. For further details regarding the GRTS algorithm, see Stevens and Olsen (2004).

After selecting a sample and collecting data, unbiased estimates of population means and totals can be obtained using the Horvitz-Thompson estimator (Horvitz and Thompson, 1952). If τ is a population total, the Horvitz-Thompson estimator for τ, denoted by $\hat{\tau}_{ht}$, is given by

$$\hat{\tau}_{ht} = \sum_{i=1}^{n} z_i \pi_i^{-1}, \tag{1}$$

where z_i is the value of the ith population unit in the sample, π_i is the inclusion probability of the ith population unit in the sample, and n is the sample size. An estimate of the population mean is obtained by dividing $\hat{\tau}_{ht}$ by N, the number of population units.

It is also important to quantify the uncertainty in $\hat{\tau}_{ht}$. The Horvitz-Thompson (Horvitz and Thompson, 1952) and Sen-Yates-Grundy (Sen, 1953; Yates and Grundy, 1953) variance estimators are often used to estimate $\text{Var}(\hat{\tau}_{ht})$, but these estimators have two drawbacks. First, they rely on calculating π_{ij}, the probability that population unit i and population unit j are both in the sample – this quantity can be challenging if not impossible to calculate analytically for GRTS samples. Second, these estimators tend to ignore the spatial locations of the population units. To address these two drawbacks simultaneously, Stevens

and Olsen (2003) proposed the local neighborhood variance estimator. The local neighborhood variance estimator does not rely on π_{ij} and estimates the variance of $\hat{\tau}$ conditional on the random properties of the GRTS sample – the idea being that this conditioning should yield a more precise estimate of $\hat{\tau}$. They show that the contribution from each sampled population unit to the overall variance is dominated by local variation. Thus the local neighborhood variance estimator is a weighted sum of variance estimates from each sampled population unit's local neighborhood. These local neighborhoods contain the sampled population unit itself and its three nearest neighbors (among all other sampled population units). For more details, see Stevens and Olsen (2003).

1.1.3. Finite Population Block Kriging

Finite population block kriging (FPBK) is a model-based approach that expands the geostatistical Kriging framework to the finite population setting (Ver Hoef, 2008). Instead of developing inference based on a specific sampling design, we assume the data are generated by a spatial stochastic process. We summarize some of the basic principles of FPBK next – see Ver Hoef (2008) for technical details and see Higham, Ver Hoef, Madsen, et al. (2021) for an extension to cases of imperfect detection among population units. Let $\mathbf{z} \equiv \{\mathrm{z}(s_1), \mathrm{z}(s_2), ..., \mathrm{z}(s_N)\}$ be an $N \times 1$ response vector at locations s_1, s_2, . . . , s_N that can be measured at the N population units. Suppose we want to use a sample to predict some linear function of the response variable, $f(\mathbf{z}) = \mathbf{b}'\mathbf{z}$, where $\mathbf{b}'$ is a $1 \times N$ vector of weights (e.g, the population mean is represented by a weights vector whose elements all equal $1/N$). Denoting quantities that are part of the sampled population units with a subscript s and quantities that are part of the unsampled population units with a subscript u, let

$$\begin{pmatrix} \mathbf{z}_s \\ \mathbf{z}_u \end{pmatrix} = \begin{pmatrix} \mathbf{X}_s \\ \mathbf{X}_u \end{pmatrix} \boldsymbol{\beta} + \begin{pmatrix} \boldsymbol{\delta}_s \\ \boldsymbol{\delta}_u \end{pmatrix}, \tag{2}$$

where $\mathbf{X}_s$ and $\mathbf{X}_u$ are the design matrices for the sampled and unsampled population units, respectively, $\boldsymbol{\beta}$ is the parameter vector of fixed effects, and $\boldsymbol{\delta} \equiv [\boldsymbol{\delta}_s \ \boldsymbol{\delta}_u]'$, where $\boldsymbol{\delta}_s$ and $\boldsymbol{\delta}_u$ are random errors for the sampled and unsampled population units, respectively.

FPBK assumes $\boldsymbol{\delta}$ in Equation (2) has mean-zero and a spatial dependence structure that can be modeled using a covariance function. This covariance function is commonly assumed to be non-negative, second-order stationary (depending only on the separation vector (e.g., distance) between population units), and isotropic (independent of direction) (Cressie, 1993). Henceforth, it is implied that we have made these same assumptions regarding $\boldsymbol{\delta}$. Chiles and Delfiner (1999), pp. 80-93 discuss covariance functions that are not second-order stationary, not isotropic, or not either. A variety of flexible covariance functions can be used to model $\boldsymbol{\delta}$ (Cressie, 1993) – one example is the exponential covariance function. Cressie (1993) provides a thorough list of spatial covariance functions. The i, jth element of the exponential covariance matrix, $\text{cov}(\boldsymbol{\delta})$, is

$$\text{cov}(\delta_i, \delta_j) = \begin{cases} \sigma_1^2 \exp(-h_{i,j}/\phi) & h_{i,j} > 0 \\ \sigma_1^2 + \sigma_2^2 & h_{i,j} = 0 \end{cases}, \tag{3}$$

where σ_1^2 is the variance parameter that quantifies the spatially dependent (correlated) variability, σ_2^2 is the variance parameter the quantifies that spatially independent (not correlated) variability, ϕ is the distance parameter that measures the distance-decay rate of the covariance, and $h_{i,j}$ is the Euclidean distance between population units i and j. In geostatistical literature, σ_1^2 is called the partial sill, σ_2^2 is called the nugget, and ϕ is called the range. We denote $\boldsymbol{\theta}$ as the

vector of covariance parameters that composes $\boldsymbol{\delta}$. In Equation 3, $\boldsymbol{\theta} = \{\sigma_1^2, \sigma_2^2, \phi\}$.

The parameters in Equation 2 can be estimated using a variety of techniques, but we focus on restricted maximum likelihood (REML) (Harville, 1977; Patterson and Thompson, 1971; Wolfinger et al., 1994). REML is preferred over maximum likelihood (ML) because ML estimates can be badly biased for small sample sizes, due to the fact that ML makes no adjustment for the simultaneous estimation of $\boldsymbol{\beta}$ and $\boldsymbol{\theta}$ (Patterson and Thompson, 1971). Minus twice the REML log-likelihood of the sampled sites is given by

$$\ln|\boldsymbol{\Sigma}| + (\boldsymbol{z}_s - \boldsymbol{X}_s\tilde{\boldsymbol{\beta}})^T\boldsymbol{\Sigma}_{ss}^{-1}(\boldsymbol{z}_s - \boldsymbol{X}_s\tilde{\boldsymbol{\beta}}) + \ln|\boldsymbol{X}_s^T\boldsymbol{\Sigma}_{ss}^{-1}\boldsymbol{X}_s| + (n-p)\ln(2\pi), \quad (4)$$

where $\tilde{\boldsymbol{\beta}} = (\boldsymbol{X}_s^T\boldsymbol{\Sigma}_{ss}^{-1}\boldsymbol{X}_s)^{-1}\boldsymbol{X}_s^T\boldsymbol{\Sigma}_{ss}^{-1}\boldsymbol{z}_s$ and $\boldsymbol{\Sigma}_{ss}$ is the covariance matrix of the sampled sites. Minimizing Equation 4 yields $\hat{\boldsymbol{\theta}}_{reml}$, the REML estimates of $\boldsymbol{\theta}$. Then $\hat{\boldsymbol{\beta}}_{reml}$, the REML estimate of $\boldsymbol{\beta}$, is given by $(\boldsymbol{X}_s^T\hat{\boldsymbol{\Sigma}}_{ss}^{-1}\boldsymbol{X})^{-1}\boldsymbol{X}_s^T\hat{\boldsymbol{\Sigma}}_{ss}^{-1}\boldsymbol{z}_s$, where $\hat{\boldsymbol{\Sigma}}_{ss}$ is $\boldsymbol{\Sigma}_{ss}$ evaluated at $\hat{\boldsymbol{\theta}}_{reml}$.

With the model formulation in Equation 2, the best linear unbiased predictor (BLUP) of $f(\mathbf{b}'\mathbf{z})$ and its prediction variance can be computed. While details of the derivation are in Ver Hoef (2008), we note here that the predictor and its variance are both moment-based, meaning that they do not rely on any distributional assumptions. Distributional assumptions are used, however, when constructing prediction intervals.

Other approaches, such as k-nearest-neighbors (Fix and Hodges, 1989; Ver Hoef and Temesgen, 2013) and random forest (Breiman, 2001), among others, could also be used to obtain predictions for a mean or total from finite population spatial data. Compared to the k-nearest-neighbors and random forest approach, we prefer FPBK because it is model-based and relies on theoretically-based variance estimators leveraging the model's spatial covariance structure, whereas k-nearest-neighbors and random forests use ad-hoc variance estimators (Ver Hoef

and Temesgen, 2013). Additionally, Ver Hoef and Temesgen (2013) compared FPBK, k-nearest-neighbors, and random forest in a variety of spatial data contexts, and FPBK tended to perform best.

2. Materials and Methods

In this section we describe how we used simulated and real data to investigate performance between simple random sampling (SRS) and GRTS sampling as well as performance between design-based (DB) and model-based (MB) inference. In SRS and GRTS sampling, all population units had equal inclusion probabilities and were selected without replacement. The important distinction between SRS and GRTS is that SRS ignores spatial locations while sampling but GRTS explicitly incorporates them. Together, the two sampling plans (SRS and GRTS) combined with the two inference approaches (DB and MB) yielded four sampling-inference combinations: SRS-DB, SRS-MB, GRTS-DB, and GRTS-MB. For SRS-DB, the Horvitz-Thompson estimator (1) was used to estimate means and the commonly-used SRS variance formula (Lohr, 2009; Särndal et al., 2003) was used to estimate variances. This variance formula is given by

$$\frac{f[\sum_{i=1}^{n}(z_i - \bar{z})^2]}{n(n-1)}, \tag{5}$$

where z_i is the response value of the ith sampled population unit, $\bar{z}$ is the mean of all z_i, n is the sample size, N is the population size, and $f = (1 - n/N)$ (f is often called the finite population correction factor). For GRTS-DB, the Horvitz-Thompson estimator was used to estimate means and the local neighborhood variance was used to estimate variances. For SRS-MB and GRTS-MB, FPBK was used to estimate means and variances using restricted maximum likelihood. SRS, GRTS sampling, and design-based inference were implemented using the `spsurvey` **R** package (Dumelle et al., 2022). FPBK was implemented using the

`sptotal` **R** package (Higham, Ver Hoef, Frank, et al., 2021).

The simulated and real data were used for distinct objectives. The simulated data was used to compare the sampling-inference combinations across many realized populations (from the same data-generating stochastic process) and random samples. The real data was used to compare the sampling-inference combinations within a single realized population but across random samples. With the simulated data, we were in control of the data-generating stochastic process and the random sampling process. With the real data, we were only in control of the random sampling process (which is typically the case in practice).

2.1. Simulated Data

We evaluated performance of the four sampling-inference combinations in 36 different simulation scenarios. The 36 scenarios resulted from the crossing of three sample sizes, two location layouts (of the population units), two response types, and three proportions of dependent random error (DRE). The three sample sizes (n) were $n = 50, n = 100$, and $n = 200$. Samples were always selected from a population size (N) of $N = 900$. The two location layouts were random and gridded. Locations in the random layout were randomly generated inside the unit square ($[0, 1] \times [0, 1]$). Locations in the gridded layout were placed on a fixed, equally spaced grid inside the unit square. The two response types were normal and skewed. For the normal response type, the response was simulated using mean-zero random errors with the exponential covariance (Equation 3) for three proportions of dependent random error (DRE): 0% DRE, 50% DRE, and 90% DRE. Recall the proportion of DRE is represented by $\sigma_1^2/(\sigma_1^2 + \sigma_2^2)$, where σ_1^2 and σ_2^2 are the DRE variance and independent random error (IRE) variance from Equation 3, respectively. The total variance, $\sigma_1^2 + \sigma_2^2$, was always 2. The distance parameter was always $\sqrt{2}/3$, chosen so that the correlation in the DRE decayed to nearly zero at $\sqrt{2}$, the largest possible distance between two population units

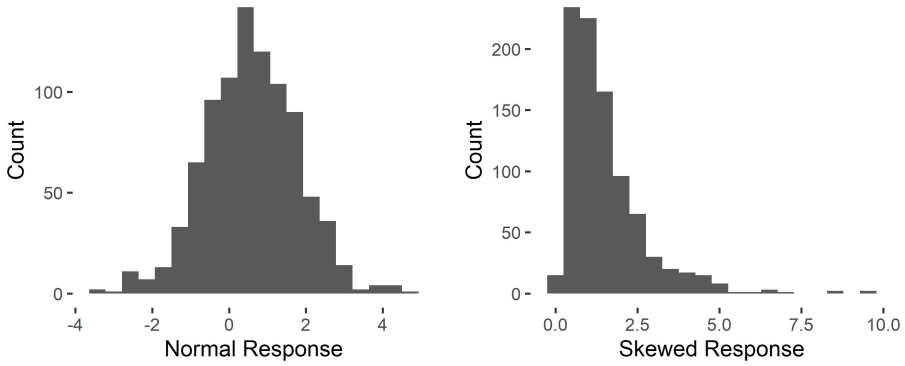

(a) Histogram of a single realized population for the normal response.

(b) Histogram of a single realized population for the skewed response.

Figure 3: Histograms of single realized populations simulated for the normal and skewed respones using the random layout and 50% DRE.

in the domain. For the skewed response type, the response was first simulated using the same approach as for the normal response type, except that the total variance was 0.6931 instead of 2. The response was then exponentiated, yielding a skewed random variable whose total variance was 2. The skewed responses were used to evaluate performance of the sampling-inference approaches for data that were not normal but were still estimated using REML, which relies on a normal log-likelihood. Figure 3 shows an example of a realized population for the normal and skewed responses using the random layout and 50% DRE.

In each of the 36 simulation scenarios, there were 2000 independent simulation trials. Within each trial, a population was simulated according to the specifications of the particular simulation scenario (for the random location layout, locations were simulated separately for each trial). Next, a random SRS sample and a random GRTS sample were selected. Then, design-based and model-based inferences were used to estimate (design-based) or predict (model-based) the realized mean and construct 95% confidence (design-based) or 95% prediction (model-based) intervals. With model-based inference, covariance parameters and the realized mean were estimated (using REML) separately for

each trial. After all 2000 trials, we summarized the long-run performance of the sampling-inference combination in each scenario by calculating mean bias, root-mean-squared error, and interval coverage. Mean bias was taken as the average deviation between each trial's estimated (or predicted) mean ($\hat{\mu}_i$) and its realized mean (μ_i): $\frac{1}{n}\sum_{i=1}^{2000}(\hat{\mu}_i - \mu_i)$, where i indexes the simulation trials. Because each trial had a different realized population, μ_i changed with i. Root-mean-squared error was taken as the square root of the average squared deviation between each trial's estimated (or predicted) mean and its realized mean: $\sqrt{\frac{1}{n}\sum_{i=1}^{2000}(\hat{\mu}_i - \mu_i)^2}$. Interval coverage was taken as the proportion of simulation trials where the realized mean was contained in its 95% confidence (or prediction) interval. These intervals were constructed using the normal distribution – justification comes from the asymptotic normality of means via the central limit theorem (under some assumptions). Quantifying these metrics is important because together, they give us an idea of the accuracy (mean bias), spread (RMSE), and validity (interval coverage) of the sampling-inference combinations.

2.2. National Lakes Assessment Data

The United States Environmental Protection Agency (USEPA), states, and tribes periodically conduct National Aquatic Research Surveys (NARS) to assess the water quality of various bodies of water in the conterminous United States. One component of NARS is the National Lakes Assessment (NLA), which measures various aspects of lake health and water quality. We focus on analyzing zooplankton multi-metric indices (ZMMI) and mercury concentrations in parts per billion (Hg ppb) from the 2012 NLA. For ZMMI, data were collected at 1035 unique lakes. At less than 10% of lakes, two ZMMI replicates were collected. These were averaged for the purposes of our study so that each lake had one measurement for ZMMI. For Hg ppb, data were collected at 995 unique lakes (there were no replicates). The ZMMI and Hg ppb data are shown as spatial

maps and as histograms in Figure 4. The ZMMI data tend to be highest near the coasts, lowest in the Central United States, are relatively symmetric, and have a mean of 55.05. The Hg ppb data tend to be highest in the Northeastern United States, lowest elsewhere, are skewed, and have a mean of 103.16 ppb. Also in Figure 4 are separate spatial semivariograms for ZMMI and Hg ppb. The spatial semivariogram quantifies the halved average squared differences (semivariance) of responses whose separation (distance) falls within a separation class. The spatial semivariance is closely related to the spatial covariance, and spatial semivariograms are often used to gauge the strength of spatial dependence in data. Both ZMMI and Hg ppb seem to have moderately strong spatial dependence (Figure 4), as the semivariance increases steadily with distance (meaning that observations nearby one another tend to be more similar than observations far apart from one another).

We studied performance of the four sampling-inference combinations by selecting 2000 SRS and GRTS samples of size $n = 50$, $n = 100$, and $n = 200$ from the realized ZMMI and Hg ppb populations and then analyzing the samples using MB and DB inference. In total, there were six separate scenarios (two responses crossed with three sample sizes). Within each SRS and GRTS sample, design-based and model-based inferences were used to estimate or predict the population mean and construct 95% coverage intervals. With model-based inference, the exponential covariance was assumed, and covariance parameters and the population mean were estimated using REML (separately for each SRS and GRTS sample). We used the same evaluation metrics as for the simulated data: mean bias, RMSE, and interval coverage. Mean bias was taken as the average deviation between each sample's estimated (or predicted) mean ($\hat{\mu}_i$) and the population mean (μ) (of ZMMI or Hg ppb): $\frac{1}{n}\sum_{i=1}^{2000}(\hat{\mu}_i - \mu)$, where i indexes the simulation trials. Because each trial had the same realized population, μ did

(a) Spatial map of the ZMMI population.

(b) Spatial map of the Hg ppb population.

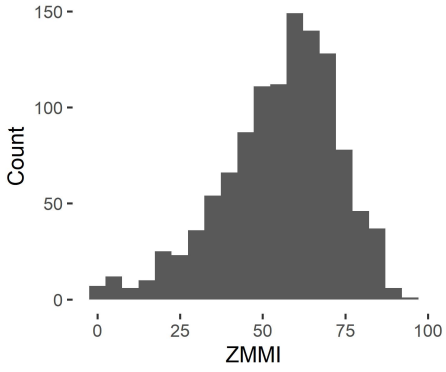

(c) Histogram of the ZMMI population.

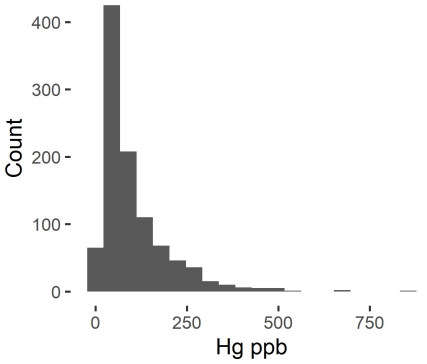

(d) Histogram of the Hg ppb population.

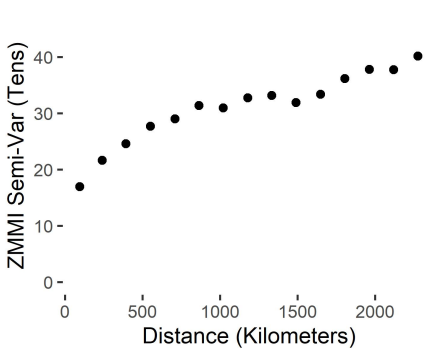

(e) Semivariogram of the ZMMI population.

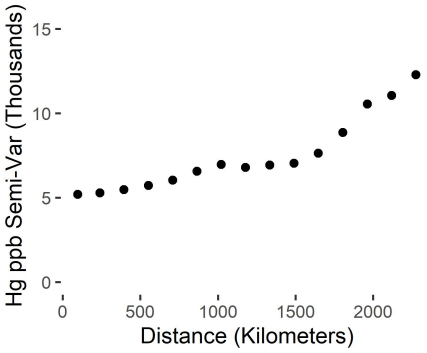

(f) Semivariogram of the Hg ppb population.

Figure 4: Exploratory graphics representing populations for the zooplankton multi-metric indices (ZMMI) and mercury concentration in parts per billion (Hg ppb) in the 2012 National Lakes Assessment (NLA) data.

not change with i (in contrast to the simulated data, where the realized mean changed with i). Root-mean-squared error was taken as the square root of the average squared deviation between each sample's estimated (or predicted) mean and its population mean: $\sqrt{\frac{1}{n}\sum_{i=1}^{2000}(\hat{\mu}_i - \mu)^2}$. Interval coverage was taken as the proportion of simulation trials where the population mean was contained in its 95% confidence (or prediction) interval. These intervals were constructed using the normal distribution.

3. Results

3.1. Simulated Data

Mean bias is nearly zero for all four sampling-inference combinations in all 36 scenarios, so we omit a more detailed summary of those results here. Tables for mean bias in all 36 simulation scenarios are provided in the supporting information.

We define the relative RMSE as a ratio with numerator given by the RMSE for a sampling-inference combination and the denominator given by the RMSE for SRS-DB. Relative RMSEs for the random location layout are provided in Fig. 5. When there is no spatial covariance (Fig. 5, "DRE%: 0%"), the four sampling-inference combinations have approximately equal RMSE. In these scenarios, using GRTS sampling or model-based inference does not generally increase efficiency compared to SRS-DB. When there is spatial covariance (Fig. 5, "DRE%: 50%" and "DRE%: 90%"), GRTS-MB tends to have the lowest RMSE, followed by GRTS-DB, SRS-MB, and finally SRS-DB. As the strength of spatial covariance increases, the gap in RMSE between SRS-DB and the other sampling-inference combinations widens. Finally we note that when there is spatial covariance, SRS-MB has a much lower RMSE than SRS-DB, suggesting that the lack of efficiency from SRS is largely mitigated by model-based inference.

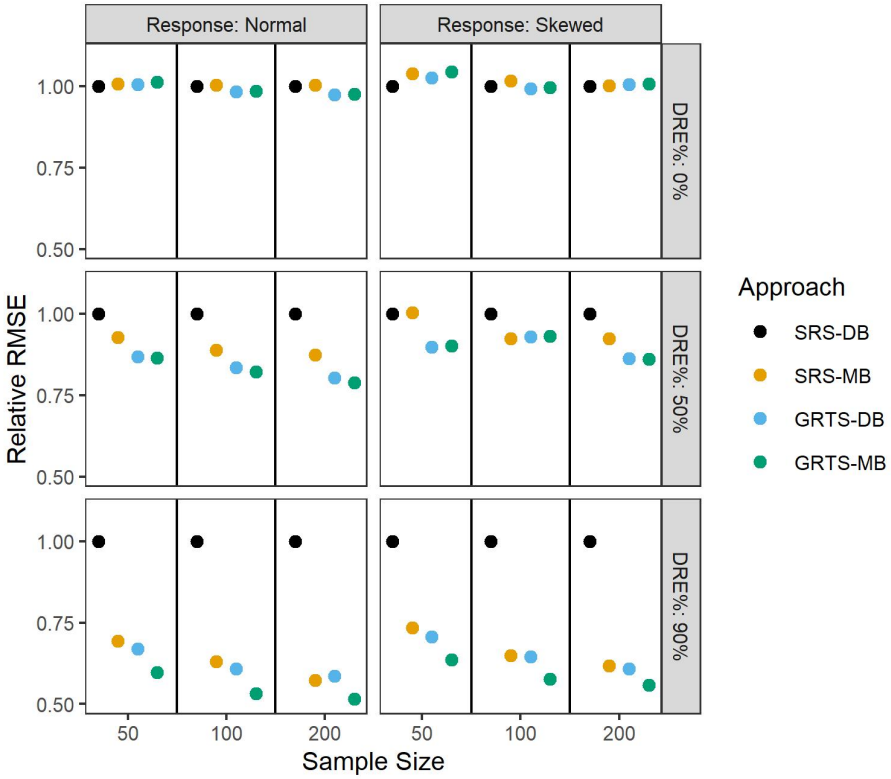

Figure 5: Simulated data relative RMSE for the four sampling-inference combinations and three sample sizes in the random location layout. The rows indicate the proportion of dependent error and the columns indicate the response type. The solid, black lines separate the sample sizes.

These RMSE conclusions are similar to those observed in the grid location layout, so we omit a figure and discussion regarding the grid location layout here. Tables for RMSE in all 36 simulation scenarios are provided in the supporting information.

95% interval coverage for each of the four sampling-inference combinations in the random location layout is shown in Fig. 6. Within each simulation scenario, all sampling-inference combinations tend to have fairly similar interval coverage, though when $n = 50$ or $n = 100$, GRTS-DB coverage is usually a few percentage points lower than the other combinations, which suggests that

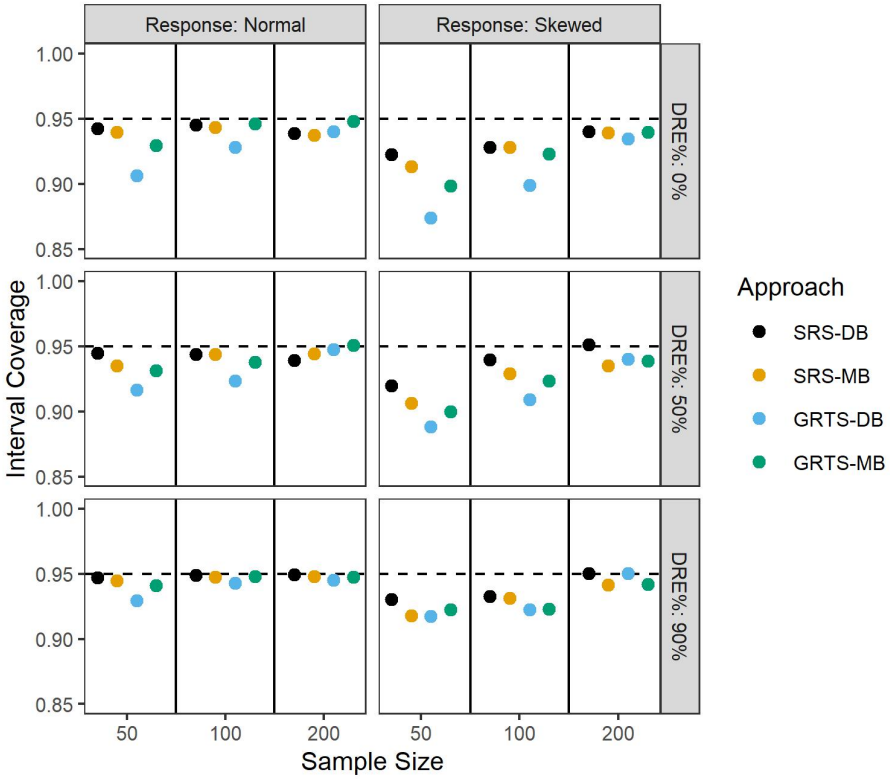

Figure 6: Simulated data interval coverage for the four sampling-inference combinations and three sample sizes in the random location layout. The rows indicate the proportion of dependent error and the columns indicate the response type. The solid black lines separate the sample sizes and the dashed black lines represent 95% coverage.

the local neighborhood variance estimate may be slightly too small for small n. Coverage in the normal response scenarios is usually near 95%, while coverage in the skewed response scenarios usually varies from 90% to 95% but increases with the sample size. At a sample size of 200, all four sampling-inference combinations have approximately 95% interval coverage in both response scenarios for all DRE proportions. These interval coverage conclusions are similar to those observed in the grid location layout, so we omit a figure and discussion regarding the grid location layout here. Tables for interval coverage in all 36 simulation scenarios are provided in the supporting information.

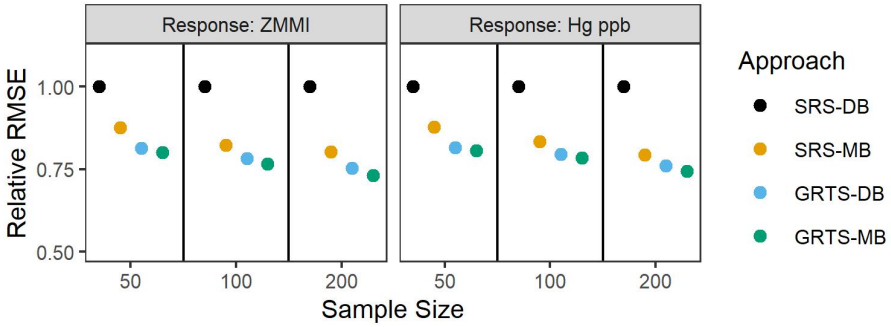

Figure 7: NLA data relative RMSE for the four sampling-inference combinations. The rows indicate the proportion of dependent error and the columns indicate the response type. The solid, black lines separate the sample sizes.

3.2. National Lakes Assessment Data

Mean bias is nearly zero for all four sampling-inference combinations in all six scenarios, so we omit a more detailed summary of those results here. Tables for mean bias in all six simulation scenarios are provided in the supporting information.

The relative RMSE of both ZMMI (symmetric response) and Hg ppb (skewed response) for all four sampling-inference combinations are shown in Fig. 7. GRTS-MB has the lowest RMSE, followed by GRTS-DB, SRS-MB, and then SRS-DB. The difference in RMSE among GRTS-MB and GRTS-DB tends to be quite small. When $n = 50$, SRS-MB RMSE is approximately evenly between SRS-DB RMSE and GRTS-MB RMSE, but for the larger sample sizes ($n = 100$, $n = 200$), SRS-MB RMSE is closer to GRTS-MB RMSE. Lastly we note that GRTS-MB, GRTS-DB, and SRS-MB all have noticeably lower RMSE than SRS-DB. Tables for RMSE in all six scenarios are provided in the supporting information.

95% interval coverage of both ZMMI and Hg ppb for all four sampling-inference combinations is shown in Fig. 8. When $n = 50$, interval coverage for both responses is too low, though interval coverage is higher for ZMMI (symmetric response) than for Hg ppb (skewed response). When $n = 100$, ZMMI interval

coverage is approximately 95% except for GRTS-DB, which has coverage around 92%, while Hg ppb interval coverage ranges from approximately 90% (GRTS-DB) to 93% (GRTS-MB). When $n = 200$, ZMMI interval coverage is approximately 95% while Hg ppb interval coverage ranges from approximately 93% (GRTS-DB) to 95% (GRTS-MB). As with the simulated data, coverages for the NLA data tend to increase with the sample sizes, coverages tend to be higher for symmetric responses than for skewed responses, and the local neighborhood variance was slightly too small for small n, yielding slightly lower interval coverages than the other sampling-inference combinations. Recall that model-based inference defines interval coverage properties across realized populations. With the simulated data, we evaluated interval coverage across realized populations, but for the NLA data, we evaluated interval coverage within a single realized population. We did find that model-based coverages were similar to the design-based coverages, however, suggesting that for some realized populations it is reasonable to heuristically view data from separate random samples as being from approximately separate realized populations. But generally, if model-based intervals constructed from many random samples of a single realized population show improper coverage, this does not necessarily imply a deficiency in model-based inference. Tables for interval coverage in all six simulation scenarios are provided in the supporting information.

4. Discussion

The design-based and model-based approaches to frequentist statistical inference rest on fundamentally different foundations. Design-based approaches rely on random sampling to estimate population parameters. Model-based approaches rely on distributional assumptions to predict realized values of a data-generating stochastic process. Though model-based approaches do not rely on random

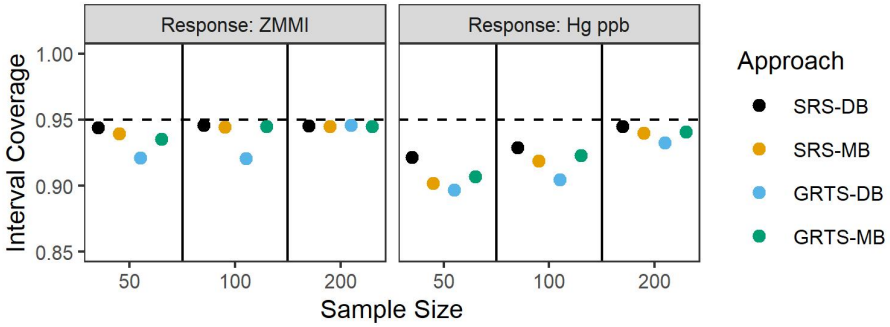

Figure 8: NLA data interval coverage for the four sampling-inference combinations. The rows indicate the proportion of dependent error and the columns indicate the response type. The solid black lines separate the sample sizes and the dashed black lines represent 95% coverage.

sampling, random sampling can still be beneficial as a way to guard against preferential sampling. While design-based and model-based approaches have often been compared in the literature from theoretical and analytical perspectives, our contribution lies in studying them for finite population spatial data while implementing GRTS sampling and the local neighborhood variance estimator. Aside from the theoretical differences described throughout the manuscript, a few analytical findings from the simulated and real data studies were particularly notable. All sampling-inference combinations had approximately zero mean bias. Independent of the inference approach, the GRTS samples yielded lower RMSE than their SRS counterparts. Though GRTS-DB and GRTS-MB generally had very similar RMSE, SRS-MB tended to have much lower RMSE than SRS-DB, suggesting that the model-based inference mitigated much of the inefficiency in RMSE from SRS. As the proportion of dependent random error in the simulated data increased, SRS-MB, GRTS-DB, and GRTS-MB become increasingly more efficient (lower RMSE) than SRS-DB. Interval coverage tended to be higher for the symmetric responses than skewed responses and tended to increase with the sample size. At a sample size of $n = 200$, generally all interval coverages were near the desired value of 95%.

There are several benefits and drawbacks of the design-based and model-based approaches for finite population spatial sampling and inference. Some we have discussed, but others we have not, and they are worthy of consideration in future research. First, we discuss advantages of the design-based approach. Design-based inference is often computationally efficient, while model-based inference can be computationally burdensome, especially for likelihood-based estimation methods like REML that rely on the inverse of a covariance matrix. Design-based inference easily handles binary data through a straightforward application of the Horvitz-Thompson estimator. In contrast, analyzing binary data using model-based inference generally requires a logistic mixed regression model, the parameters of which can be difficult to estimate and interpret (Bolker et al., 2009). An advantage of design-based inference is that interval coverage is valid (has the proper coverage rate) as long as 1) the sample is sufficiently large to ensure the statistic's sampling distribution is approximately normal and 2) the variance estimator is consistent (Brus and De Gruijter, 1997; Särndal et al., 2003). This is because with the design-based approach, the sampling plan and inclusion probabilities are specified directly by the researcher. An advantage of SRS-DB not previously mentioned is that it is likely to be valid given the consistency of its variance estimator (Särndal et al., 2003). With the model-based approach, however, interval coverage is unlikely to be valid if the model assumptions made do not not accurately reflect reality. Whether model assumptions accurately reflect reality can be a challenging and sometimes impossible question to answer definitively.

Now, we discuss advantages of the model-based approach. The model-based approach can more naturally quantify the relationship between covariates (predictor variables) and the response variable than design-based approaches. Model-based inference also yields estimated spatial covariance parameters, which

help better understand the dependence structure of the process in study. Model selection is also possible using model-based inference and criteria such as cross validation, likelihood ratio tests, or AIC (Akaike, 1974). Model-based inference is capable of more efficient small-area estimation than design-based inference because model-based inference can leverage distributional assumptions in areas with few observed population units. Model-based approaches also accommodate unit-by-unit predictions at unobserved locations that can be used to construct informative visualizations like smoothed maps. Brus and De Gruijter (1997) provide a more thorough discussion regarding the benefits and drawbacks of the two approaches. In short, when deciding whether the design-based or model-based approach is more appropriate to implement, these benefits and drawbacks should be considered alongside the particular goals of the study.

There are many extensions of this research worthy of future consideration that include sampling with unequal inclusion probabilities, using different spatially balanced sampling approaches (instead of GRTS), using different spatial data configurations, using different spatial domains like stream networks (Ver Hoef and Peterson, 2010), using different response or covariance structures, and using spatial or external mean trends (which can be defined through covariates).

Acknowledgments

We would like to thank the editors and anonymous reviewers for their hard work and time spent providing us with thoughtful, valuable feedback which greatly improved the manuscript.

The views expressed in this manuscript are those of the authors and do not necessarily represent the views or policies of the U.S. Environmental Protection Agency or the National Oceanic and Atmospheric Administration. Any mention of trade names, products, or services does not imply an endorsement by the

U.S. government, the U.S. Environmental Protection Agency, or the National Oceanic and Atmospheric Administration. The U.S. Environmental Protection Agency and National Oceanic and Atmospheric Administration do not endorse any commercial products, services, or enterprises.

Conflict of Interest Statement

There are no conflicts of interest for any of the authors.

Author Contribution Statement

All authors conceived the ideas; All authors designed the methodology; MD and MH performed the simulations and analyzed the data; MD and MH led the writing of the manuscript; All authors contributed critically to the drafts and gave final approval for publication.

Data and Code Availability

This manuscript has a supplementary **R** package that contains all of the data and code used in its creation. The supplementary **R** package is hosted on GitHub. Instructions for download are available at

https://github.com/michaeldumelle/DvMsp.

If the manuscript is accepted, this repository will be archived in Zenodo.

Supporting Information

In the supporting information, we provide tables of summary statistics for all 36 simulation scenarios and all six real data scenarios.

References

Akaike, H., 1974. A new look at the statistical model identification. IEEE Transactions on Automatic Control 19, 716–723.

Barabesi, L., Franceschi, S., 2011. Sampling properties of spatial total estimators under tessellation stratified designs. Environmetrics 22, 271–278.

Benedetti, R., Piersimoni, F., 2017. A spatially balanced design with probability function proportional to the within sample distance. Biometrical Journal 59, 1067–1084.

Benedetti, R., Piersimoni, F., Postiglione, P., 2017. Spatially balanced sampling: A review and a reappraisal. International Statistical Review 85, 439–454.

Bolker, B.M., Brooks, M.E., Clark, C.J., Geange, S.W., Poulsen, J.R., Stevens, M.H.H., White, J.-S.S., 2009. Generalized linear mixed models: A practical guide for ecology and evolution. Trends in ecology & evolution 24, 127–135.

Breiman, L., 2001. Random forests. Machine Learning 45, 5–32.

Brus, D., De Gruijter, J., 1997. Random sampling or geostatistical modelling? Choosing between design-based and model-dased sampling strategies for soil (with discussion). Geoderma 80, 1–44.

Brus, D.J., 2021. Statistical approaches for spatial sample survey: Persistent misconceptions and new developments. European Journal of Soil Science 72, 686–703.

Brus, D.J., DeGruijter, J.J., 1993. Design-based versus model-based estimates of spatial means: Theory and application in environmental soil science. Environmetrics 4, 123–152.

Chan-Golston, A.M., Banerjee, S., Handcock, M.S., 2020. Bayesian inference for finite populations under spatial process settings. Environmetrics 31, e2606.

595 Chiles, J.-P., Delfiner, P., 1999. Geostatistics: Modeling Spatial Uncertainty.
596 John Wiley & Sons, New York.

597 Cicchitelli, G., Montanari, G.E., 2012. Model-assisted estimation of a spatial
598 population mean. International Statistical Review 80, 111–126.

599 Cooper, C., 2006. Sampling and variance estimation on continuous domains.
600 Environmetrics 17, 539–553.

601 Cressie, N., 1993. Statistics for spatial data. John Wiley & Sons.

602 De Gruijter, J., Ter Braak, C., 1990. Model-free estimation from spatial
603 samples: A reappraisal of classical sampling theory. Mathematical Geology 22,
604 407–415.

605 Diggle, P.J., Menezes, R., Su, T.-l., 2010. Geostatistical inference under
606 preferential sampling. Journal of the Royal Statistical Society: Series C (Applied
607 Statistics) 59, 191–232.

608 Dumelle, M., Kincaid, T.M., Olsen, A.R., Weber, M.H., 2022. Spsurvey:
609 Spatial sampling design and analysis.

610 Fix, E., Hodges, J.L., 1989. Discriminatory analysis. Nonparametric dis-
611 crimination: Consistency properties. International Statistical Review/Revue
612 Internationale de Statistique 57, 238–247.

613 Grafström, A., 2012. Spatially correlated poisson sampling. Journal of
614 Statistical Planning and Inference 142, 139–147.

615 Grafström, A., Lundström, N.L., 2013. Why well spread probability samples
616 are balanced. Open Journal of Statistics 3, 36–41.

617 Grafström, A., Lundström, N.L., Schelin, L., 2012. Spatially balanced
618 sampling through the pivotal method. Biometrics 68, 514–520.

619 Grafström, A., Matei, A., 2018. Spatially balanced sampling of continuous
620 populations. Scandinavian Journal of Statistics 45, 792–805.

621 Hansen, M.H., Madow, W.G., Tepping, B.J., 1983. An evaluation of model-

dependent and probability-sampling inferences in sample surveys. Journal of the American Statistical Association 78, 776–793.

Harville, D.A., 1977. Maximum likelihood approaches to variance component estimation and to related problems. Journal of the American Statistical Association 72, 320–338.

Higham, M., Ver Hoef, J., Frank, B., Dumelle, M., 2021. Sptotal: Predicting totals and weighted sums from spatial data.

Higham, M., Ver Hoef, J., Madsen, L., Aderman, A., 2021. Adjusting a finite population block kriging estimator for imperfect detection. Environmetrics 32, e2654.

Hofman, S.C., Brus, D., 2021. How many sampling points are needed to estimate the mean nitrate-n content of agricultural fields? A geostatistical simulation approach with uncertain variograms. Geoderma 385, 114816.

Horvitz, D.G., Thompson, D.J., 1952. A generalization of sampling without replacement from a finite universe. Journal of the American Statistical Association 47, 663–685.

Lohr, S.L., 2009. Sampling: Design and analysis. Nelson Education.

Patterson, H.D., Thompson, R., 1971. Recovery of inter-block information when block sizes are unequal. Biometrika 58, 545–554.

Robertson, B., Brown, J., McDonald, T., Jaksons, P., 2013. BAS: Balanced acceptance sampling of natural resources. Biometrics 69, 776–784.

Robertson, B., McDonald, T., Price, C., Brown, J., 2018. Halton iterative partitioning: Spatially balanced sampling via partitioning. Environmental and Ecological Statistics 25, 305–323.

Särndal, C.-E., Swensson, B., Wretman, J., 2003. Model assisted survey sampling. Springer Science & Business Media.

Schabenberger, O., Gotway, C.A., 2017. Statistical methods for spatial data

649 analysis. CRC press.

650 Sen, A.R., 1953. On the estimate of the variance in sampling with varying
651 probabilities. Journal of the Indian Society of Agricultural Statistics 5, 127.

652 Sterba, S.K., 2009. Alternative model-based and design-based frameworks
653 for inference from samples to populations: From polarization to integration.
654 Multivariate Behavioral Research 44, 711–740.

655 Stevens, D.L., Olsen, A.R., 2003. Variance estimation for spatially balanced
656 samples of environmental resources. Environmetrics 14, 593–610.

657 Stevens, D.L., Olsen, A.R., 2004. Spatially balanced sampling of natural
658 resources. Journal of the American Statistical Association 99, 262–278.

659 USEPA, 2012. National lakes assessment 2012. https://www.epa.gov/national-
660 aquatic-resource-surveys/national-results-and-regional-highlights-national-lakes-
661 assessment.

662 Ver Hoef, J., 2002. Sampling and geostatistics for spatial data. Ecoscience 9,
663 152–161.

664 Ver Hoef, J.M., 2008. Spatial methods for plot-based sampling of wildlife
665 populations. Environmental and Ecological Statistics 15, 3–13.

666 Ver Hoef, J.M., Peterson, E.E., 2010. A moving average approach for spatial
667 statistical models of stream networks. Journal of the American Statistical
668 Association 105, 6–18.

669 Ver Hoef, J.M., Temesgen, H., 2013. A comparison of the spatial linear
670 model to nearest neighbor (k-nn) methods for forestry applications. PlOS ONE
671 8, e59129.

672 Walvoort, D.J., Brus, D., De Gruijter, J., 2010. An r package for spatial
673 coverage sampling and random sampling from compact geographical strata by
674 k-means. Computers & geosciences 36, 1261–1267.

675 Wang, J.-F., Jiang, C.-S., Hu, M.-G., Cao, Z.-D., Guo, Y.-S., Li, L.-F., Liu, T.-

J., Meng, B., 2013. Design-based spatial sampling: Theory and implementation. Environmental Modelling & Software 40, 280–288.

Wolfinger, R., Tobias, R., Sall, J., 1994. Computing gaussian likelihoods and their derivatives for general linear mixed models. SIAM Journal on Scientific Computing 15, 1294–1310.

Yates, F., Grundy, P.M., 1953. Selection without replacement from within strata with probability proportional to size. Journal of the Royal Statistical Society: Series B (Methodological) 15, 253–261.